

Supplementary information for

Structure of Liquid/Liquid interface during Solvent Extraction combining X-ray and Neutron Reflectivity Measurements

E. Scoppola, E. Watkins, G. Li Destri, L. Porcar, R. A. Campbell, O. Konovalov, G. Fragneto and O. *Diat

Corresponding Author: olivier.diat@cea.fr

SI.1: Experimental cells

Two cells were developed for x-ray and neutron reflectivity experiments and a schematic view is presented in figure SI.1.

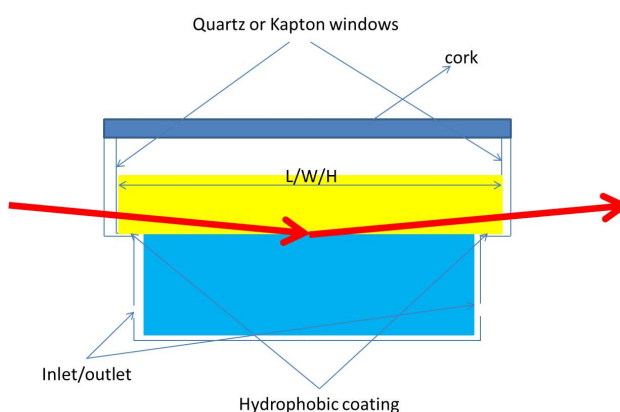


Figure SI.1. The cells are composed of two adjacent compartments, the lower one for the aqueous phase and the upper one for the organic phase. The upper one is longer and larger and a step separates both parts. This step has an hydrophobic coating in order to prevent the aqueous phase covering this horizontal section. Thus the borders of the meniscus are fixed to the edges and the meniscus is minimized by adding or removing the aqueous solution using the inlet or outlet with a connected syringe. Windows are made of quartz or Kapton® depending on the radiation used. The length (L) is approximately 50 or 70 mm for the neutron and x-ray beams, respectively. The cell depth (H) is few centimeters as well as the width (W). The diamide concentration can be changed from the top of the cell.

SI.2: X-ray and neutron reflectivity measurements

Neutron reflectivity experiments were performed and possible thanks to the unique 'reflection down' option on the versatile time-of-flight reflectometer, FIGARO, at the Institut Laue-Langevin (Grenoble, France).¹ Neutrons of wavelengths between 2.5 and 16 Å and at two different angles, 0.617° and 1.4°,

were used to obtain a Q-range from 0.01 \AA^{-1} to 0.15 \AA^{-1} . The neutron reflectivity profiles, $R_N(Q)$, are plotted using the ratio between the reflected beam and the direct beam through the sample.

X-ray reflectivity experiments were performed on the ID10 beamline at ESRF (Grenoble, France) with energy of 22 keV. The x-ray reflectivity beam, $R_X(Q)$, was recorded as a function of the incident angle (or wave vector Q) normalized by the direct beam through the sample (at 0 angle).

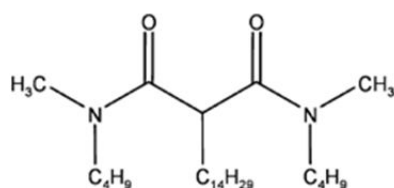
The momentum transfer Q is defined by

$$Q = \frac{4\pi}{\lambda} \sin(\theta)$$

where θ is the incident angle.

For both experiments the data have been analyzed using Motofit² and a Parratt analysis (see §SI.4) which allows the fitting of the experimental data to produce corresponding SLD profiles. The analysis of the reflectivity profiles using a uniform layer model of constant electron or nuclear density is questionable; we eliminated all possibilities of lateral inhomogeneities at the interface due to possible patchy organizations of the extractants and ions complexes (the complex being neutral) and due to concentration fluctuations by working below and at the CAC, and thus we can assume a rather homogeneous lateral distribution of species at the interface but stratified perpendicularly to the interface.

SI.3: Malonamide molecule



DMDBTDMA

Figure SI.2. DMDBTDMA or N1,N3-dimethyl-N1,N3-dibutyl-2-tetradecyl-malonamide scheme

DMDBTDMA was obtained from Pharmasynthese (France) with purity higher than 99 %. The extractant was purified using the following process: 0.5 M of diamide in pentane was first prepared and an alumina (Prolabo 32.101.290) column already washed with pentane was filled with the solution. 100 ml of this solution was then eluted on 10 g of basic alumina. Then the pentane was evaporated with a Rotovapor at 35 °C. Dodecane (99 %) was supplied by Sigma-Aldrich (France). It was distilled in an all-glass apparatus and passed seven times through an alumina column to remove any active impurities.⁵⁰

Solutions of extractant in dodecane were precontacted with water before filling the reflectivity cells

Ultrapure water (Milli-Q Labo, Millipore) was used. 65% nitric acid purum was purchased from Aldrich and also used as received. Deuterated dodecane (D26) was supplied by Eurisotop (France).

SI.4: Parratt analysis

In the following tables and graphs we show the convenience of using two instead of one layer for analyzing our x-ray reflectivity data at various diamide concentrations:

0.02 M diamide– assumption of 1 Layer

	Thickness (Å)	SLD (10^{-6} \AA^{-2})	Roughness (Å)
Organic phase	-	7.38	-
1 st layer	17.5	11.3	5.6
Aqueous phase	-	10.6	9.5

Table SI.1. fitting parameters in the Motofit procedure for data adjustment plotted in figure SI.3 left.

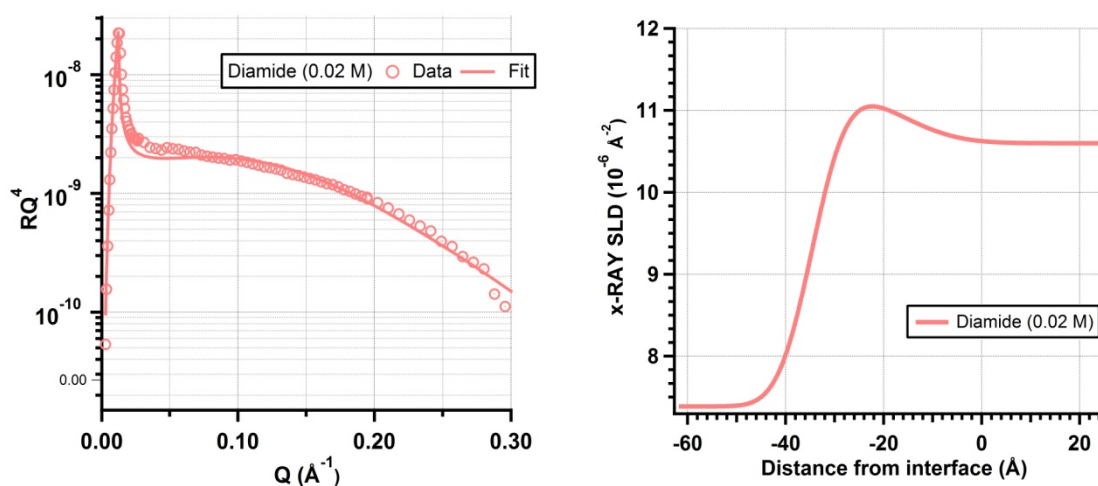


Figure SI.3. (Left) X-ray reflectivity curves in the RQ^4 vs Q representation for the 2M LiNO_3 , 0.25M NdNO_3 water solution - dodecane interface in presence of 0.02M diamide with the fitting curve using a Parratt procedure. (Right) SLD profiles as a function of depth perpendicular to the water/oil interface for 0.02M diamide concentration and obtained from x-ray measurements fitting (left graph) using a 1-layer model with parameters listed in the table above. The organic phase corresponds to the negative z -values and the aqueous phase to the positives.

The curvature of the intensity decrease is not very well reproduced; a two-layer model in the Parratt procedure was then applied with the fitting parameter listed in the table below.

0.02 M diamide– assumption of 2-Layers

	Thickness (Å)	SLD (10^{-6} Å^{-2})	Roughness (Å)
Organic phase	-	7.38	-
1st layer	23.8	8.3	7.9
2 nd layer	19.0	12.1	5.7
Aqueous phase	-	10.6	7.9

Table SI.2. Fitting parameters in the Motofit procedure for x-ray data adjustment plotted in figure 1 of the main article (0.02 M for diamide concentration).

0.07 M diamide– assumption of 1-Layers

	Thickness (Å)	SLD (10^{-6} Å^{-2})	Roughness (Å)
Organic phase	-	7.39	-
1 st layer	21.1	11.4	6.3
Aqueous phase	-	10.6	36.0

Table SI.3. Fitting parameters in the Motofit procedure for x-ray data adjustment plotted in figure SI.4 left.

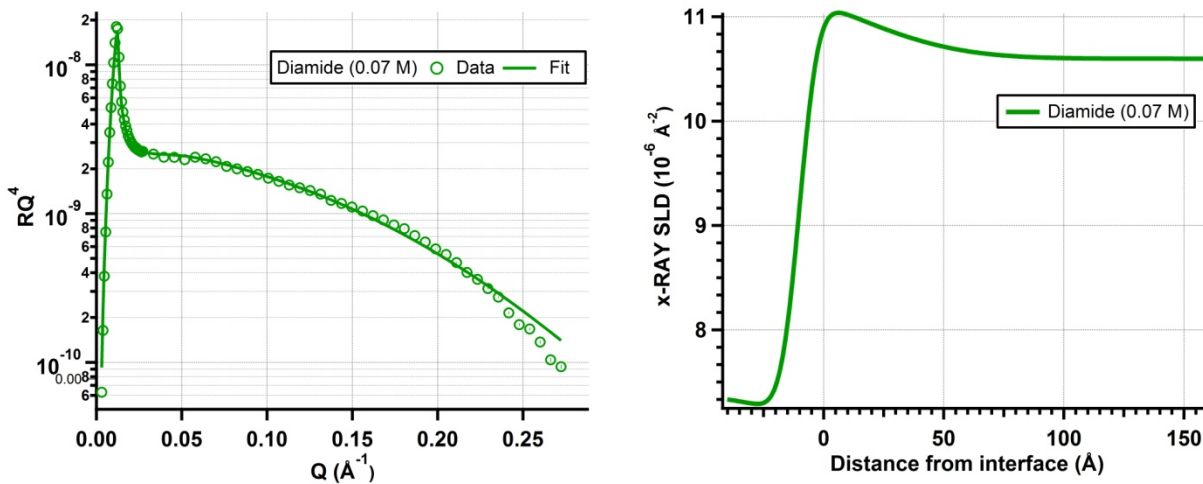


Figure SI.4. (Left) X-ray reflectivity curves in the RQ^4 vs Q representation for the 2M LiNO₃, 0.25M NdNO₃ water solution - dodecane interface in presence of 0.07M diamide with the fitting curve using a Parratt procedure. (Right) SLD profiles as a function of depth perpendicular to the water/oil interface for 0.07M diamide concentration and obtained from x-ray measurements fitting (left graph) using a 1-layer model with parameters listed in the table above. The organic phase corresponds to the negative z-values and the aqueous phase to the positives.

To force the reflectivity curve adjustment (see figure SI.4 left) and to describe the intensity decrease, a rather large roughness has to be taken into account which is not physical for an interfacial tension of about 15 mN/m.

If we fix the water phase roughness to be smaller and closer to the nominal value (6-10 \AA), then the fit is not acceptable (see the following graph SI.5).

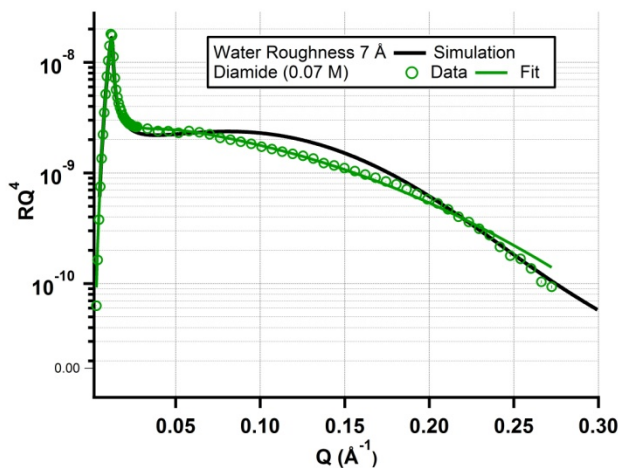


Figure SI.5. X-ray reflectivity curves in the RQ^4 vs Q representation for the 2M LiNO₃, 0.25M NdNO₃ water solution - dodecane interface in presence of 0.07M diamide with the fitting curve using a Parratt procedure (with parameters listed in the table above but fixing a "water" roughness to a value smaller than 10 \AA).

0.07 M diamide– assumption of 2-Layers

	Thickness (Å)	SLD (10^{-6} Å^{-2})	Roughness (Å)
Organic phase	-	7.39	-
1st layer	6.8	14.3	8.3
2nd layer	33.1	10.9	7.9
Aqueous phase	-	10.6	7.9

Table SI.4. Fitting parameters in the Motofit procedure for x-ray data adjustment plotted in figure 1 of the main article (0.02 M for diamide concentration).

The fitting adjustments listed in this table are those used in the fitting adjustment shown in figure 1 of the main article (x-ray data).

Same procedure for the reflectivity measurements adjustment can be applied for higher concentrations in diamide.

The variation of the interfacial roughness only is not sufficient to analyze accurately the modulation and intensity decrease of our reflectivity measurements.

SI. 5: Monte-Carlo Sampling

To determine the distribution profile of each species across the organic/aqueous interface, we developed a Fortran code for Monte Carlo sampling of the location of the ions and molecules. This approach allowed us to analyze the SLD profiles obtained with the Motofit fitting process. Samples contained 6 species (water, neodymium and lithium nitrate salts, dodecane and diamide) and so 6 equations are needed to solve the concentration profile as a function of depth. There are 2 equations related to experimental data from neutron and x-ray reflectivity measurements, and there are 4 other equations related to various constraints that are used to have the full set of equations. These constraints are related to the ion concentrations and to the total charge that should be minimized. The initial conditions are a gradient of concentration between the organic phase with dodecane and the diamide on one side and the salt solution on the other side.

Completely different initial conditions were tested (i.e. starting from a homogeneous distribution of each species) and similar profiles were obtained (see fig SI.3).

For the code some quantities are defined and listed in the supplementary information as well as details of the fittings procedure (see SI.4 and tables SI.1 and SI.2).

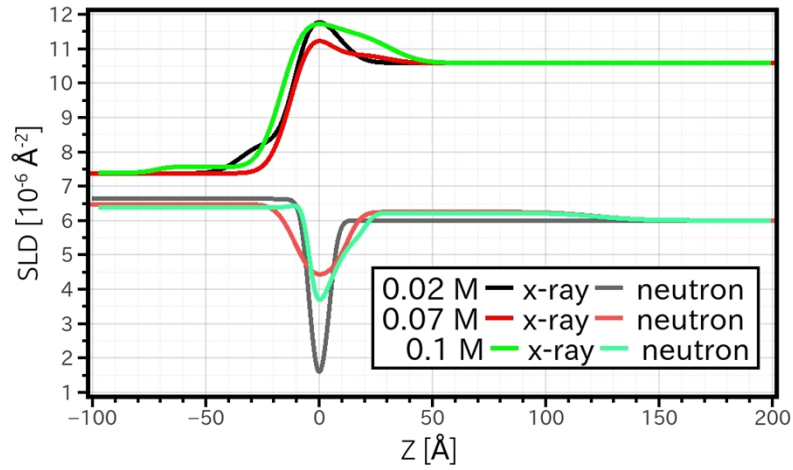


Figure SI.6. Alignment of the 6 SLD profiles: for each concentration where maxima of the x-ray profiles and the minima of the neutron profiles are arbitrarily fixed at $z=0$. On the left the bulk organic phase is represented, on the right the bulk aqueous phase.

For the code some quantities are defined and listed in table SI.5.

Type of molecule in the system	$\alpha_j, j=1,6$
Type of atoms for each molecule species	$n_{\alpha_j}, j=1,6$
Experimental and theoretical number of molecules for each species in each z	$N_{\alpha_j,exp}(z), N_{\alpha_j,theo}(z)$
Number of molecules for each z	$N_{\alpha}(z) = \sum_{j=1}^6 N_{\alpha_j}(z)$
Experimental or simulated molecular volume for each component	$v_{i,m,exp}(z), v_{i,m,simul}(z)$
Experimental x-ray SLD for each z	$\rho_{x,exp}(z) = \frac{\sum_{j=1}^6 N_{\alpha_j,exp}(z) \sum_{l=1}^{n_{\alpha_j}} Z_l(z) r_l}{\sum_{j=1}^6 N_{\alpha_j,exp}(z) v_{j,m,exp,x}(z)}$
Experimental neutron SLD for each z	$\rho_{n,exp}(z) = \frac{\sum_{j=1}^6 N_{\alpha_j,exp}(z) \sum_{l=1}^{n_{\alpha_j}} b_l(z)}{\sum_{j=1}^6 N_{\alpha_j,exp}(z) v_{j,m,exp,n}(z)}$

Simulated x-ray SLD for each z	$\rho_{x,simul}(z) = \frac{\sum_{j=1}^6 N_{\alpha_j,simul}(z) \sum_{l=1}^{n_{\alpha_j}} Z_l(z)}{\sum_{j=1}^6 N_{\alpha_j,simul}(z) v_{j,m,simul}(z)}$
Simulated neutron SLD for each z	$\rho_{n,simul}(z) = \frac{\sum_{j=1}^6 N_{\alpha_j,simul}(z) \sum_{l=1}^{n_{\alpha_j}} b_l(z)}{\sum_{j=1}^6 N_{\alpha_j,simul}(z) v_{j,m,simul}(z)}$
Experimental molecular volume (in \AA^3) for each z for neutrons and x-rays	$v_{m,exp,n}(z) = \sum_{j=1}^6 N_{\alpha_j,exp}(z) v_{j,m,exp,n}(z)$ $v_{m,exp,x}(z) = \sum_{j=1}^6 N_{\alpha_j,exp}(z) v_{j,m,exp,x}(z)$
Simulated molecular volume (in \AA^3) for each z for neutrons and x-rays	$v_{m,simul,n}(z) = \sum_{j=1}^6 N_{\alpha_j,simul}(z) v_{j,m,simul,n}(z)$ $v_{m,simul,x}(z) = \sum_{j=1}^6 N_{\alpha_j,simul}(z) v_{j,m,simul,x}(z)$

Table SI.5. Basic equations to calculate the scattering length density for x-ray and neutron probes.

We fix the total volume for each z as:

$$v_{m,exp,x}(z) = 87030 \text{\AA}^3$$

Samples with the same composition were used for x-ray and neutron experiments.

For the Monte Carlo sampling we generate randomly different $N_{\alpha_j}(z)$ and for each set we calculate the molecular volume for neutron samples as followed:

$$v_{m,exp,n}(z) = \frac{\sum_{j=1}^6 N_{\alpha_j}(z) v_{j,m,simul,n}(z)}{\sum_{j=1}^6 N_{\alpha_j}(z) v_{j,m,simul,x}(z)} \cdot v_{m,exp,x}(z) = \frac{\sum_{j=1}^6 N_{\alpha_j}(z) v_{j,m,simul,n}(z)}{\sum_{j=1}^6 N_{\alpha_j}(z) v_{j,m,simul,x}(z)} \cdot 87030 \text{\AA}^3$$

to take into account the different volume for hydrogenous and deuterated samples.

The scattering length density was calculated using:

$$\rho_{j,x,simul}(z) = \sum_{l=1}^{n_{\alpha_j}} Z_l(z) r_l$$

and

$$\rho_{j,n,simul}(z) = \sum_{l=1}^{n_{\alpha_j}} b_l(z)$$

The values for all the species in the system are reported in table SI.6.

If we know the composition of each layer we should minimize the following difference, which is independent of the molar volumes:

$$\frac{\rho_{x,simul}(z)}{\rho_{n,simul}(z)} - \frac{\rho_{x,exp}(z)}{\rho_{n,exp}(z)} = \epsilon(z)$$

or

$$\frac{\sum_{j=1}^6 N_{\alpha_j,simul}(z) \sum_{l=1}^{n_{\alpha_j}} Z_l(z) r_l}{\sum_{j=1}^6 N_{\alpha_j,simul}(z) \sum_{l=1}^{n_{\alpha_j}} b_l(z)} - \frac{\rho_{x,exp}(z)}{\rho_{n,exp}(z)} = \epsilon(z)$$

and also the differences for each experiment:

$$\frac{\sum_{j=1}^6 N_{\alpha_j,simul}(z) \sum_{l=1}^{n_{\alpha_j}} Z_l(z) r_l}{v_{m,exp,x}(z)} - \rho_{x,exp}(z) = \gamma(z)$$

$$\frac{\sum_{j=1}^6 N_{\alpha_j,simul}(z) \sum_{l=1}^{n_{\alpha_j}} b_l(z)}{v_{m,exp,n}(z)} - \rho_{n,exp}(z) = \delta(z)$$

After 10^6 loops in the code, several sets of three $\epsilon(z)$, $\gamma(z)$ and $\delta(z)$ that match, according to the fixed constraints, are produced. Those that respect the following conditions are kept.

$$|\epsilon_{min}(z) \cdot -\epsilon_i(z)| \leq 0.01 \cdot \epsilon_{min}(z)$$

$$|\gamma_{min}(z) \cdot -\gamma_i(z)| \leq 0.01 \cdot \gamma_{min}(z)$$

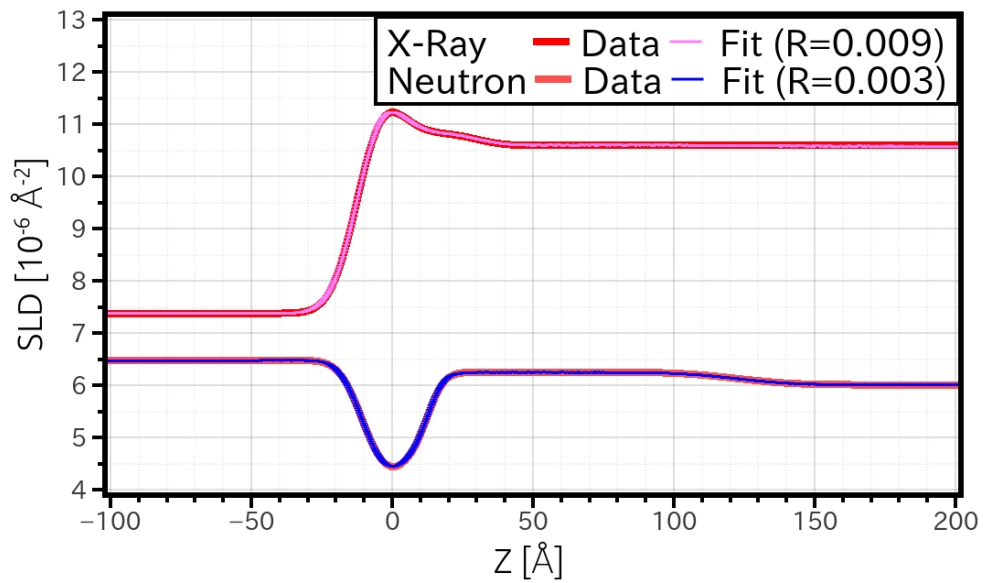
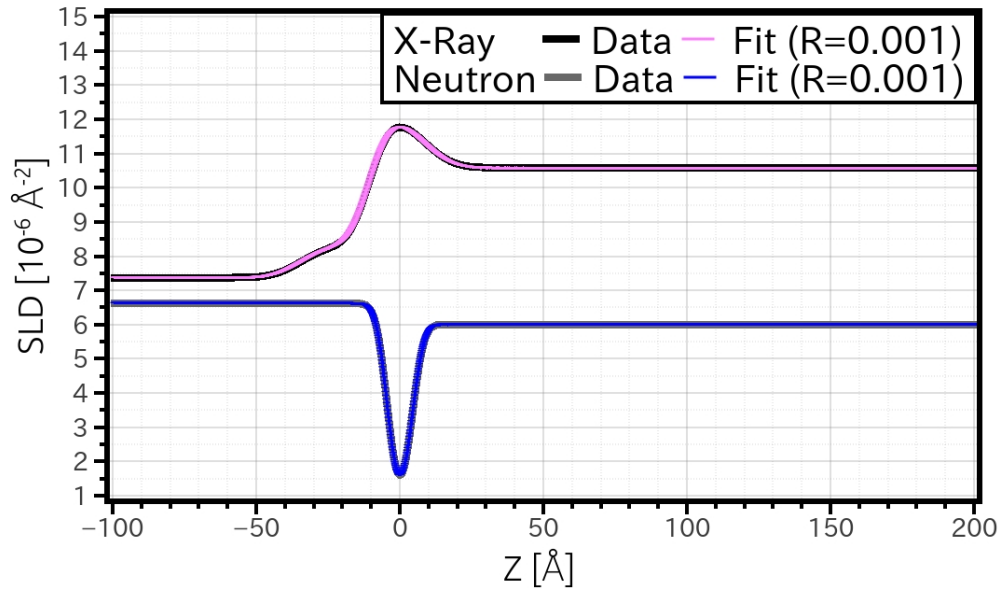
$$|\delta_{min}(z) \cdot -\delta_i(z)| \leq 0.01 \cdot \delta_{min}(z)$$

Then the corresponding $N_{\alpha_j,teo}(z)$ are averaged and the total procedure is repeated 600 times.

At the end, the quality of the fit for each data is described by a parameter R defined as follows:

$$R = \sqrt{\frac{\sum_{i=1}^{n_{slice}} \left(\frac{\rho_{exp}(z_i) - \rho_{theo}(z_i)}{\rho_{exp}(z_i)} \right)^2}{n_{slice}}}$$

and the simulated SLD solutions are reported in figures SI.7 (up, medium, down) and superimposed to the data stemmed from the Motofit program.



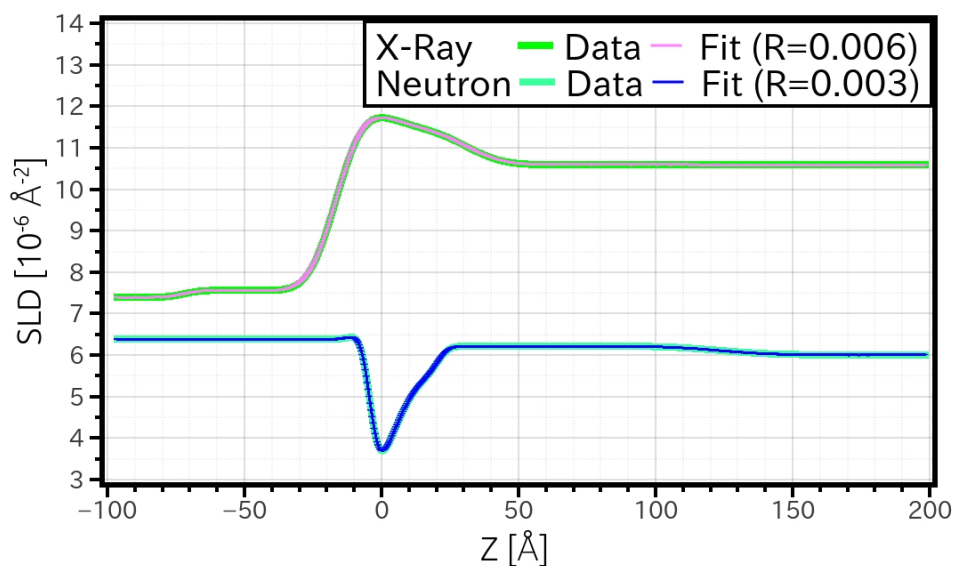


Figure SI.7.SLD profiles for (up) 0.02 M (medium) 0.07M and (down) 0.1M of diamide concentration.

Species	Scattering Length (10^{-6}\AA)		Scattering Length Density (10^6\AA^{-2})		Molecular volume
	X-Ray	Neutron	X-Ray	Neutron	
DMDBTDMA	6951.9	79.31	8.654	0.0979	803.25
$C_{12}H_{26}$	2768.3	-174.33	7.291	-0.459	379.66
$C_{12}D_{26}$	2768.3	2533.0	7.330	6.707	377.67
H_2O	238.2	-16.73	9.419	-0.564	30.07
D_2O	283.2	191.53	9.366	6.334	30.23
Li	84.54	-0.19	/	/	/
NO_3	878.6	267.75	/	/	/
Nd	1606.6	76.9	/	/	/
$D_2O + 2M LiNO_3 +$	/	/	10.59	6.02	/

Table SI.6. Scattering length and scattering length density of each species in the samples. For the mixture $D_2O + 2M LiNO_3 + 0.25 M Nd(NO_3)_3$ we report the SLD values obtained using x-ray and

neutron reflectivity measurements. For the calculation of the scattering length we used a molecular volume equal to 1 \AA^3 .

The error bars around the averaged data for each species distribution at various diamide concentrations are displayed in figures below; averaged data come from the overall distributions that meet the defined criteria:

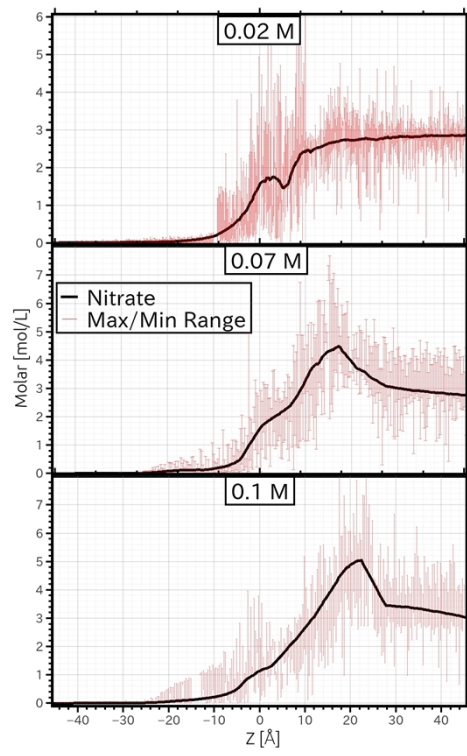
$$|\epsilon_{min}(z) - \epsilon_i(z)| \leq 0.01 \cdot \epsilon_{min}(z)$$

$$|\gamma_{min}(z) - \gamma_i(z)| \leq 0.01 \cdot \gamma_{min}(z)$$

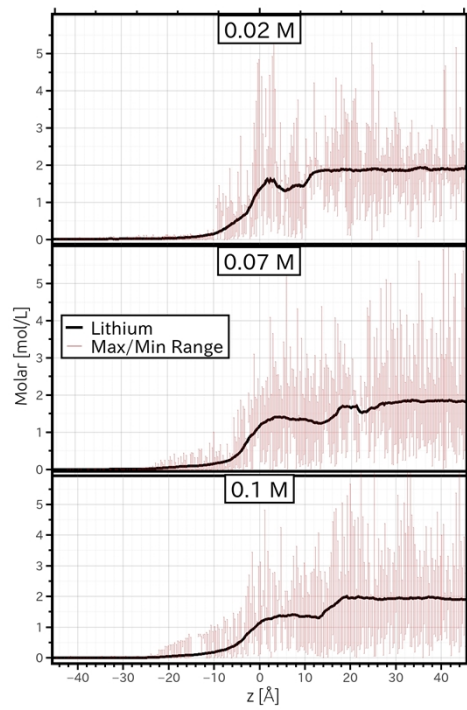
$$|\delta_{min}(z) - \delta_i(z)| \leq 0.01 \cdot \delta_{min}(z)$$

See next the distributions of nitrate (a), neodinium (b) and lithium (c) ions across the W/O interface for three diamide concentrations – same curves than those presented in the main article but with error bars:

a)



b)



c)

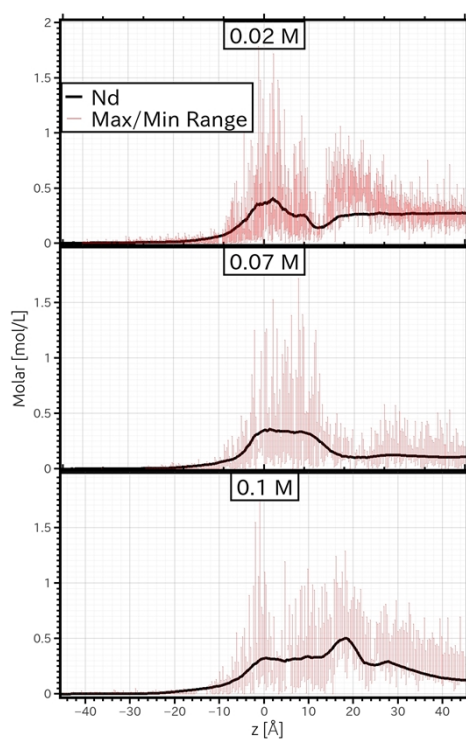


Figure SI8. Density profiles across the liquid/liquid interface at three concentrations of diamide in the organic phase.

- 1 R. A. Campbell, H. P. Wacklin, I. Sutton, R. Cubitt and G. Fragneto, *European Physical Journal Plus*, 2011, **126**.
- 2 A. Nelson, *Journal of Applied Crystallography*, 2006, **39**, 273.